J Mater Sci: Mater Med (2007) 18:1945–1954
DOI 10.1007/s10856-007-3097-3

Formation of calcium phosphates on titanium implants with four different bioactive surface preparations. An in vitro study

Anna Arvidsson · Victoria Franke-Stenport · Martin Andersson · Per Kjellin · Young-Taeg Sul · Ann Wennerberg

Received: 21 November 2005 / Accepted: 12 June 2006 / Published online: 7 June 2007

Abstract The aim of the present study was to compare the nucleating and growing behaviour on four types of bioactive surfaces by using the simulated body fluid (SBF) model. Titanium discs were blasted and then prepared by alkali and heat treatment, anodic oxidation, fluoridation, or hydroxyapatite coating. The discs were immersed in SBF for 1, 2, 4 and 6 weeks. Calcium phosphates were found on all specimens, as analysed with scanning electron microscopy/energy dispersive X-ray analysis (SEM/EDX). After 1 and 2 weeks of SBF immersion more titanium was accessible with SEM/EDX on the blasted surfaces than the four bioactive surface types, indicating a difference in coverage by calcium phosphates. The Ca/P mean ratio of the surfaces was approximately 1.5 after 1 week, in contrast to the fluoridated specimens which displayed a Ca/P mean ratio of approximately 2. Powder X-ray diffraction (P-XRD) analyses showed the presence of hydroxyapatite on all types of surfaces after 4 and 6 weeks of immersion. The samples immersed for 6 weeks showed a higher degree of crystallinity than the samples immersed for 4 weeks. In conclusion, differences appeared at the early SBF immersion times of 1 and 2 weeks between controls and bioactive surface types, as well as between different bioactive surface types.

A. Arvidsson (✉) · V. Franke-Stenport · Y.-T. Sul · A. Wennerberg
Department of Biomaterials, Institute of Surgical Sciences, Göteborg University, Box 412, Goteborg 405 30, Sweden
e-mail: anna.arvidsson@biomaterials.gu.se

V. Franke-Stenport · A. Wennerberg
Department of Prosthetic Dentistry/Dental Technology, Göteborg University, Box 450, Goteborg 405 30, Sweden

M. Andersson · P. Kjellin
Department of Applied Surface Chemistry, Chalmers University, Goteborg 412 96, Sweden

Introduction

The clinical outcome of dental and orthopaedic implants is dependent on sufficient bone anchorage, which is generally considered to be obtained by biomechanical and biochemical anchorage mechanisms [1]. Titanium implants are anchored to bone through in growth between and into small irregularities of the implant surface, so called biomechanical interlocking. In the case of a threaded design, the threads will provide additional biomechanical support. Biochemical bonding is potentially obtained by bioactive implants; Hench has defined bioactivity as ''the characteristic of an implant material which allows it to form a bond with living tissues'' [2]. According to Osborn and Newesly [3] titanium is bioinert in contrast to bioactive materials such as various calcium phosphates and bioglasses. Theoretically, the advantage with bioactive implants is that biochemical attachment is rapid, i.e., it acts at a time when proper biomechanical interlocking has not yet been developed, and consequently the implants may be fixed earlier.

Bone formation around titanium implants is not fully understood. For example, some studies have reported that bone appears to grow gradually towards the implant surface [4, 5], while others have reported bone growth directly on the titanium surface [6, 7]. Other authors have concluded that bone formation occurs in two directions; bone does not only approach the biomaterial, but also grows from the implant towards the healing bone [8–10]. Fur-

thermore, little is known about the biochemical bond at the chemical level of possible bioactive implants.

In order to understand the bone anchorage mechanisms better, the ultrastructure of the bone titanium interface has been investigated. Early observations were limited to decalcified specimens [11, 12] due to technical difficulties with preparation [13]. In 1992 Sennerby et al. [14] resolved the intact interface zone at solid titanium implants for the first time on un-decalcified specimens with a fracture technique developed by Linder [15] and Thomsen and Ericson [16]. At areas with direct mineralised bone-titanium contact at the light microscopic level, the implant surface was separated from the mineralised bone with a 100–200 nm thick amorphous granular layer with no hydroxyapatite crystals present [14]. However, they could not exclude the possibilities that calcium could be present in the amorphous layer in any other form, or that hydroxyapatite was dissolved from it during the preparation procedure [17]. Furthermore, they observed an approximately 100 nm thick layer with a higher electron density between the mineralised bone and the amorphous layer [14]. Different constituents of the amorphous layer have been reported, including proteoglycans [18, 19], osteopontin [8] and osteocalcin [20].

The interface between bone and materials other than titanium has also been compared and ultrastructural differences have been reported [18, 21]. However, there still remain many questions concerning the bonding mechanisms between bone and titanium substrates with different surface treatments.

The bone–implant interface has also been studied in vitro with bone marrow cells, and morphological similarities with the bone–biomaterial interface developed in vivo were reported [6, 22]. Another in vitro model extensively used to investigate bone formation is immersion of the biomaterial in simulated body fluids (SBF), solutions with ion concentrations approximately equal to those of human blood plasma [23–28]. Depending on the nucleating capacity of the material, bone-like calcium phosphates have precipitated onto the surface. Immersion time is one factor found to influence the amount, and the crystalline degree, of the calcium phosphate precipitate [29].

In order to enhance the bone formation around titanium, surface modifications with respect on topography have been performed [30–34]. A surface roughness of approximately 1.5 μm has been reported as optimal for bone anchorage when comparing blasted titanium implants with different surface roughnesses [33, 35–37]. Some authors have in a first step increased the surface roughness (e.g., with etching, plasma spraying or blasting), and in a second step chemically modified the surface with the goal to obtain bioactivity [38–41]. That approach was also selected in the present study; after increasing the roughness with a blasting procedure the specimens were subjected to alkali and heat treatment [42], anodic oxidation [43], fluoridation [44], or hydroxyapatite [45]. It has been impossible to prove bioactivity so far, but different indications for bioactivity have been presented for the above mentioned surface treatments [1]. For example, a bone like apatite layer has been formed to alkali and heat treated titanium when immersed in SBF [46]. Furthermore, when fluoridated or anodically oxidised implants have been removed from rabbit bone, the rupture has generally occurred in the bone tissue and not at the bone to implant interface [43, 44]. Bioactive properties of hydroxyapatite coated implants have been reviewed by LeGeros [47].

However, several surface treatments not only affect the chemistry but also other surface properties such as oxide thickness, porosity and topography. For example, alkali treatment of titanium results in a porous gel layer of sodium titanate that becomes more mechanically stable after the heat treatment [42]. The anodic oxidation procedure also increases the porosity, as well as the oxide thickness [48]. Fluoride treatment has been reported to result in surface topography changes as well [49].

Since titanium surfaces modified with different preparation techniques have different surface properties, it can be hypothesised that the different surfaces will exhibit different nucleating and bone bonding properties. The above mentioned surface modifications of titanium have previously been investigated with the SBF model to various degrees. However, studies comparing calcium phosphate precipitation on different surfaces claimed to be bioactive are still lacking. Therefore, the aim of the present study was to compare the nucleating and growing behaviour of those four different types of surfaces, suggested as bioactive, by using the SBF model.

Materials and methods

Surface preparations

In total 90 circular discs (Ø: 8 mm, thickness: 3 mm) of commercially pure titanium (grade 3) were included in the present study. In order to increase the surface roughness, the specimens were blasted with Al_2O_3 powder with a particle size of 75 μm. Thereafter, the specimens were ultrasonically cleaned in diluted Extran MA01 and absolute ethanol, respectively, and dried at 60 °C for 24 h. The specimens were then divided into five groups, among which one group ($n = 18$) served as a control and was not subjected to any surface treatment prior to the SBF immersion. The other groups of specimens were treated with the following surface preparations.

Alkali and heat treatment

Alkali and heat treatment was performed as described in the literature [25, 42, 50]. The specimens (n = 18) were soaked in 5 M aqueous NaOH for 24 h at 60 °C and were thereafter gently washed with distilled water before they were let to dry for 24 h at 40 °C. The specimens were then heated to 600 °C by increasing the temperature by 5 °C/min in air an electrical furnace (Bitatherm, Bita Laboratory Furnaces, Israel), and were kept at 600 °C for 1 h before being allowed to cool to room temperature in the furnace.

Anodic oxidation

Samples (n = 18) were prepared in a mixed electrolyte containing magnesium ions such as magnesium sulphate using the Micro Arc Oxidation (MAO) method in galvanostatic mode [51]. The electrochemical cell was composed of two platinum plates as cathodes and the titanium anode at the centre. Currents and voltages were continuously recorded at intervals of one second by an IBM computer interfaced with a DC power supply. The content of ripple was controlled to less than 0.1%. The surface properties of the oxidised group were characterized as a magnesium titanate consisting of some 9 at% Mg, 3.4 μm of oxide thickness, 24% porosity of porous structure, anatase plus rutile of crystal structure [52].

Fluoridation

One group of specimens (n = 18) was fluoridated as per the technique of Ellingsen [44]: the specimens were immersed in an aqueous solution of 0.95 M NaF and subsequently washed twice in distilled water for 30 s. The specimens were then allowed to dry spontaneously at room temperature. X-ray photoelectron spectroscopy (XPS) was used to confirm the presence of fluorine.

Hydroxyapatite coating

A hydroxyapatite coating was obtained by dipping the titanium discs (n = 18) into a stable sol which contained surfactants, water, organic solvent and crystalline nanoparticles of hydroxyapatite with a Ca/P ratio of 1.67. The diameter of the hydroxyapatite particles was approximately 10 nm. After the dipping procedure the discs were dried for half an hour in open air, allowing the organic solvent to evaporate. This was followed by a heat treatment at 550 °C for 5 min under nitrogen atmosphere in order to remove all dispersing agents. The nitrogen atmosphere protected the titanium surface from further oxidation. The treatment resulted in a very thin hydroxyapatite coat on the titanium surface (less than 100 nm thick), as measured with XPS.

SBF immersion

The revised SBF (r-SBF) described by Oyane et al. [53] was used in the present study. It was prepared by dissolving 5.403 g NaCl, 0.740 g $NaHCO_3$, 2.046 g Na_2CO_3, 0.225 g KCl, 0.230 g $K_2HPO_4 \cdot 3H_2O$, 0.311 g $MgCl_2 \cdot 6H_2O$, 11.928 g 2-(4-(2-hydroxyethyl)-1-piperazinyl)ethanesulfonic acid (HEPES), 0.293 g $CaCl_2$, and 0.072 g Na_2SO_4 in 1,000 mL distilled water. HEPES was dissolved in 100 mL distilled water before being added to the solution, and the final pH was adjusted to 7.4 at 37 °C with 1.0 M NaOH.

Each specimen was immersed in 25 mL r-SBF in separate sealed polystyrene vials and kept at 37 °C. Once every week the r-SBF was changed to freshly prepared buffer. After immersion for 1 week (3 samples), 2 weeks (3 samples), 4 weeks (3 samples), and 6 weeks (6 samples) the SBF immersion was interrupted and the specimens were thoroughly rinsed with distilled water to remove any loosely attached calcium phosphate material. The specimens were then dried at room temperature and sealed in dry vials whilst awaiting surface analysis. Three samples of each type of surface were not immersed in any SBF, thus serving as controls within each surface preparation group.

Evaluation of surfaces

Weight

The weight change of each specimen due to the SBF immersion was calculated by measuring the dry weight before and after SBF immersion with an analytical balance (HR-200, A&D Instruments, UK), which has a repeatability of 0.1 mg.

Contact stylus profilometry

All specimens were topographically analysed after SBF immersion with a contact stylus profilometer (Surfascan 3J®, Somicronic, France), and the specimens of each surface type that were not immersed in SBF were used as controls. The analysis was performed over a measuring area of 0.5×0.5 mm^2, with 4 μm between scans and a stylus radius of 2 μm. Each disc was measured in one area, located in the corresponding region for all discs regardless of group.

A Gaussian filter with size 80×80 μm^2 was applied to separate roughness from form and waviness. Thereafter the surface roughness, in terms of the following topographical parameters, was calculated:

S_a = Arithmetic mean height deviation from a mean plane [μm].

S_{ds} = Density of summits, i.e. the number of summits of a unit sampling area [mm^{-2}].
S_{dr} = Developed interfacial area ratio, i.e. the ratio of the increment of the interfacial area of a surface over the sampling area [%].

Mathematical descriptions of the parameters can be found in the literature [54].

Scanning electron microscopy/energy dispersive X-ray analysis (SEM/EDX)

For the SEM analyses, a LEO Ultra 55 FEG SEM equipped with an Oxford Inca EDX system, operating at 7 kV, was used. The samples were examined without surface sputtering. Micrographs were recorded at different magnifications to investigate both the surface coverage and the morphologies of the crystals. The atomic composition was monitored using EDX analysis on two scales. Analyses at a low magnification were performed on a major part of the sample to describe a mean value of the atomic composition. Analyses on individual crystals were also made in order to identify them by correlating their structure with their chemical composition.

Powder X-ray diffraction (P-XRD)

In order to investigate the crystallinity and crystal structure of the precipitate formed after immersion in SBF for 4 and 6 weeks, powder X-ray diffraction was performed with a Siemens D5000 X-ray diffractometer equipped with a CuKα radiation source with a wavelength of 1.54 Å. Scans were collected in the range of 20–60° (2θ). Specimens immersed in SBF for 1 and 2 weeks were not investigated with P-XRD since the amount of material was insufficient.

Results

Weight

In general, the alkali and heat treated, fluoridated, and hydroxyapatite coated specimens increased their weight after SBF immersion, while a weight loss tendency was noted for some of the blasted and anodically oxidised specimens (Table 1).

Contact stylus profilometry

The results from the topographic surface analysis demonstrated that the mean values at baseline were rather similar for S_a, S_{ds} and S_{dr} parameters with small differences between the various surface treatments. However, the anodically oxidised surface had an S_{dr} mean value approximately 50% higher than the other surfaces. The standard deviation in this group was also higher than the other groups.

S_a mean values

The mean value decreased after 1, 2, and 4 weeks compared to baseline means. After 6 weeks the mean values were higher in all groups compared to the baseline mean values.

S_{ds} mean values

The results demonstrated lower mean values after 1 and 2 weeks compared to the baseline mean values. At 4 and 6 weeks the mean values were close to the baseline means but not higher.

S_{dr} mean values

In general the mean values varied more from one time interval to another compared to the other surface parameters and the standard deviations were higher in several groups. Most of the groups demonstrated a similar trend with a decrease compared to baseline at 1, 2 and 4 weeks. All groups demonstrated higher mean values after 6 weeks compared to controls.

For details see Table 2.

SEM/EDX

The blasted controls and the hydroxyapatite coated controls had a rough surface with sharp edges before SBF immersion, while the morphology of the alkali and heat treated, anodically oxidised and the fluoridated controls was more divergent from each other (Fig. 1). The alkali and heat treated surface displayed structures with smoother edges (Fig. 1B), while the anodically oxidised specimens displayed an increased porosity (Fig. 1C). Small flake structures could be seen on the fluoridated specimens (Fig. 1D).

One week of SBF immersion

Calcium phosphates were found on all specimens. The crystals displayed a porous structure with sharp angled edges (Fig. 2), and a Ca/P ratio of approximately 1.3. Sodium sulphate (Na_2SO_4) was also detected on the anodically oxidised, alkali and heat treated and the hydroxyapatite coated specimens. All samples except the blasted had approximately 10–15 at% titanium on the surface (Fig. 3). The blasted specimens had a titanium

Table 1 Weight changes of the specimens before and after SBF immersion

SBF immersion time	*N*	Δ Weight (after – before SBF immersion) (mg)				
		B	AH	AO	F	HA
1 week	3	0.4 (1.4)	0.1 (0.4)	–44.3 (40.1)	4.1 (4.2)	2.3 (4.0)
2 weeks	3	–0.7 (2.1)	<0.1 (0.3)	–13.5 (15.7)	0.2 (0.8)	0.2 (0.2)
4 weeks	3	–13.2 (14.6)	1.4 (0.5)	–10.8 (21.1)	1.1 (0.6)	1.8 (1.9)
6 weeks	6	1.2 (8.0)	4.5 (1.3)	–2.2 (8.7)	3.1 (0.9)	3.0 (0.3)

B: blasted titanium, AH: alkali and heat treated, AO: anodically oxidised, F: fluoridated, and HA: hydroxyapatite coated. The figures represent mean values, standard deviations within parenthesis

Table 2 Topographical results as measured with contact stylus profilometry

SBF immersion time	Suface type	*n*	S_a (μm)	S_{ds} (mm^{-2})	S_{dr} (%)
0 weeks	B	3	0.62 (0.14)	1725 (128)	1.36 (0.42)
	AH	3	0.63 (0.02)	1571 (98)	1.55 (0.08)
	AO	3	0.73 (0.22)	1600 (209)	2.57 (1.72)
	F	3	0.71 (0.09)	1512 (37)	1.66 (0.55)
	HA	3	0.75 (0.19)	1671 (92)	1.93 (0.65)
1 week	B	3	0.52 (0.01)	1650 (93)	0.96 (0.12)
	AH	3	1.11 (0.98)	1583 (64)	8.99 (13.55)
	AO	3	0.58 (0.09)	1321 (92)	0.93 (0.30)
	F	3	0.68 (0.05)	1479 (90)	1.47 (0.11)
	HA	3	0.99 (0.38)	1465 (52)	3.12 (2.10)
2 weeks	B	3	0.52 (0.14)	1727 (100)	1.06 (0.50)
	AH	3	0.58 (0.05)	1583 (64)	1.30 (0.20)
	AO	3	0.58 (0.11)	1369 (269)	1.00 (0.16)
	F	3	0.67 (0.09)	1527 (17)	1.52 (0.40)
	HA	3	0.70 (0.03)	1745 (80)	1.57 (0.06)
4 weeks	B	3	0.63 (0.43)	1704 (288)	2.75 (3.41)
	AH	3	0.54 (0.02)	1610 (147)	1.24 (0.14)
	AO	3	0.60 (0.04)	1369 (269)	2.14 (1.72)
	F	3	1.08 (0.51)	1575 (32)	6.82 (4.96)
	HA	3	0.59 (0.06)	1614 (109)	1.30 (0.20)
6 weeks	B	6	2.52 (2.30)	1523 (193)	34.23 (41.35)
	AH	6	3.97 (3.56)	1453 (309)	55.62 (62.62)
	AO	6	1.35 (0.71)	1544 (83)	10.05 (10.03)
	F	6	1.13 (0.69)	1552 (167)	8.84 (12.41)
	HA	6	1.27 (0.43)	1670 (118)	8.60 (5.52)

B: blasted titanium, AH: alkali and heat treated, AO: anodically oxidised, F: fluoridated, and HA: hydroxyapatite coated. The figures represent means, standard deviations within parenthesis

content of approximately 30 % on the surface. The calcium phosphates detected had a Ca/P mean ratio of about 1.5, but on the fluoridated samples the Ca/P mean ratio was approximately 2 (Fig. 4).

Two weeks

No Na_2SO_4 could be detected on any sample. The blasted titanium surfaces still had approximately 30 at% titanium, and the other surface types about 10–15 at%. The crystals formed had the same appearance as after 1 week immersion (Fig. 5).

Four weeks

All specimens were covered by calcium phosphates after 4 weeks of immersion, with a surface mean Ca/P ratio of approximately 2. Spherical crystals were detected on a

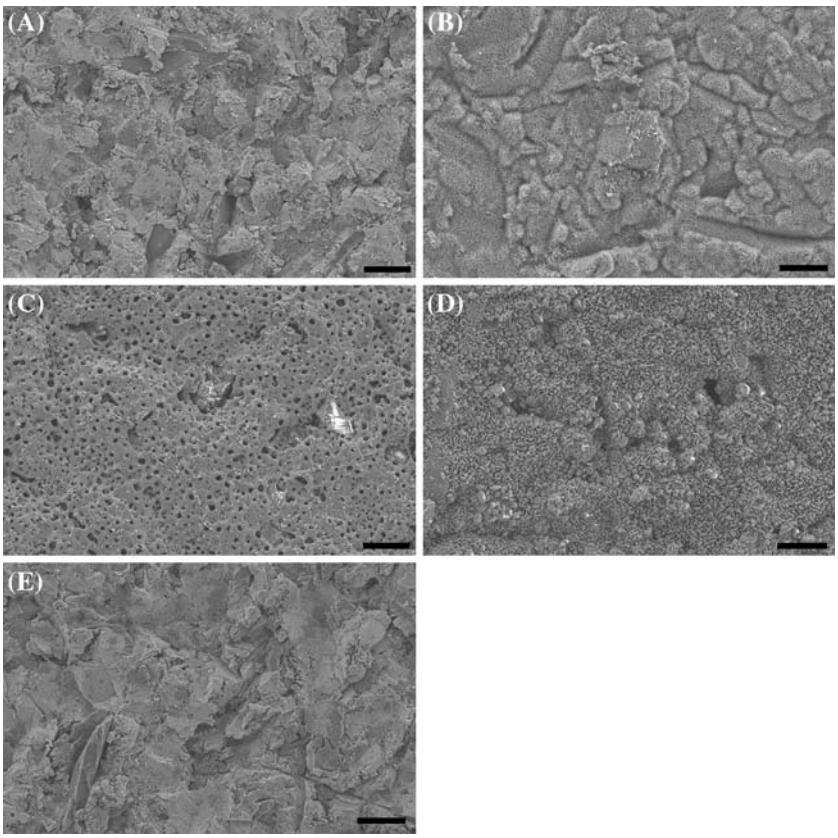

Fig. 1 SEM images of the surfaces before SBF immersion. (**A**) blasted, (**B**) alkali and heat treated, (**C**) anodically oxidised, (**D**) fluoridated, and (**E**) HA coated (bars = 10 μm)

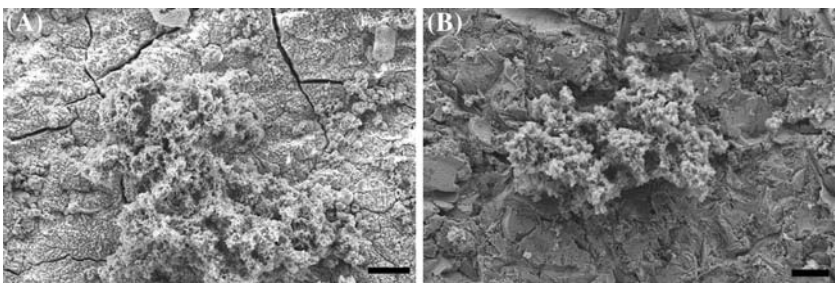

Fig. 2 SEM images of structures after 1 week SBF immersion on (**A**) a fluoridated specimen (bar = 10 μm) and (**B**) a hydroxyapatite coated specimen (bar = 10 μm)

tightly packed layer with cracks that had been formed (Fig. 6). The compact layer had a Ca/P ratio of about 1.6 and the spherical crystals of about 2.0.

Six weeks

After 6 weeks immersion all surfaces were completely covered by calcium phosphates (Fig. 7). The Ca/P mean ratios of the surfaces increased to slightly more than 2.

P-XRD

After 4 weeks immersion XRD signals were detected from titanium and hydroxyapatite (Fig. 8A), and after 6 weeks SBF immersion, the hydroxyapatite signals became narrower and the titanium signals were less intense (Fig. 8B). Furthermore, after 4 weeks SBF immersion the signal was increased at lower degrees ($2\theta < 25°$) for all surface types, which was not seen in the diffractograms after 6 weeks of immersion. This shows that the precipitate formed on the 4 week samples is more amorphous than the 6 week samples.

Discussion

In the present study the formation of calcium phosphates on titanium implants with various surface preparations claimed to be bioactive, was investigated with the same settings in an SBF model. Calcium phosphates were formed on all surfaces, but some differences were indicated. The calcium phosphates formed on the fluoridated

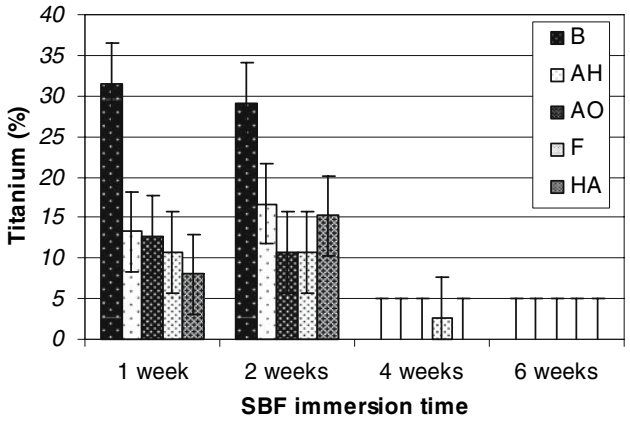

Fig. 3 Titanium amounts from EDX analyses. B: blasted titanium, AH: Alkali and heat treated, AO: anodically oxidised, F: fluoridated, and HA: HA coated. The bars are based on means, calculated from two 3 mm^2 large measurement areas from two different specimens

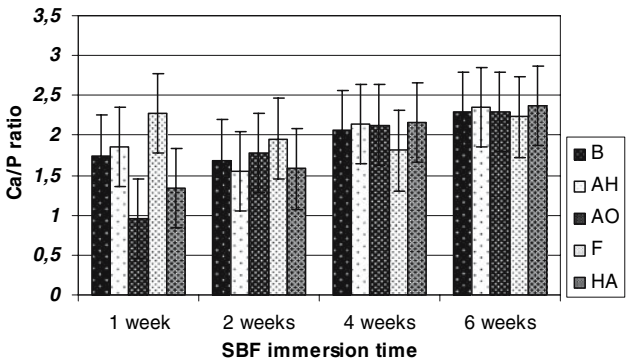

Fig. 4 Ca/P ratios from EDX analyses. B: blasted titanium, AH: Alkali and heat treated, AO: anodically oxidised, F: fluoridated, and HA: HA coated. The staples are based on means, calculated from two 3 mm^2 large measurement areas of two different specimens

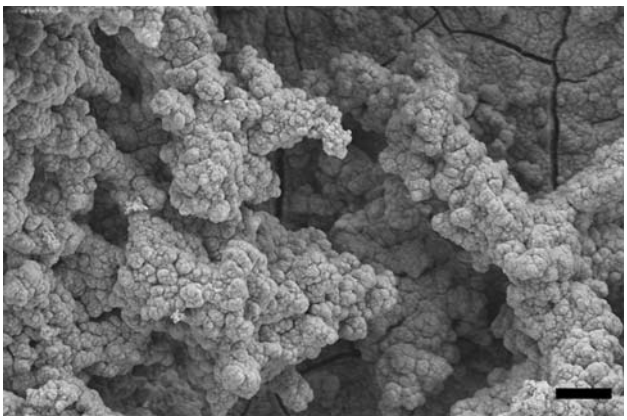

Fig. 6 A SEM image of a fluoridated specimen immersed in SBF for 4 weeks (bar = 10 μm)

specimens diverged by exhibiting a high Ca/P ratio at an early stage.

Previously, the precipitation of calcium phosphates on surfaces has been studied in vitro using a variety of solutions, including SBF with varying compositions. In the present study a revised SBF [53] was chosen with an electrolyte concentration very similar to that of human plasma [55]. Regardless of the buffer used, it should be stressed that it is a simplified model for the conditions in vivo. For example, human blood plasma contains other components not included in the SBF, such as proteins, cells and gases like carbon dioxide. However, a simplified model can facilitate the understanding of the initial phase of bone formation around titanium implants. It is also possible to increase the complexity of the model, i.e. to increase the similarity with bone formation. By doing so it

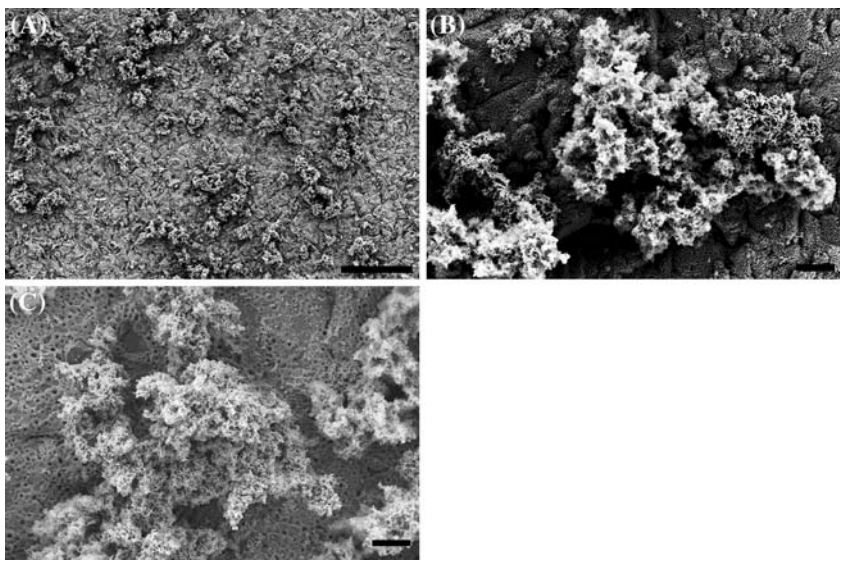

Fig. 5 SEM images of specimens after two weeks of SBF immersion. (**A**) blasted (bar = 100 μm), (**B**) alkali and heat treated (bar = 10 μm), (**C**) anodically oxidised surface (bar = 10 μm)

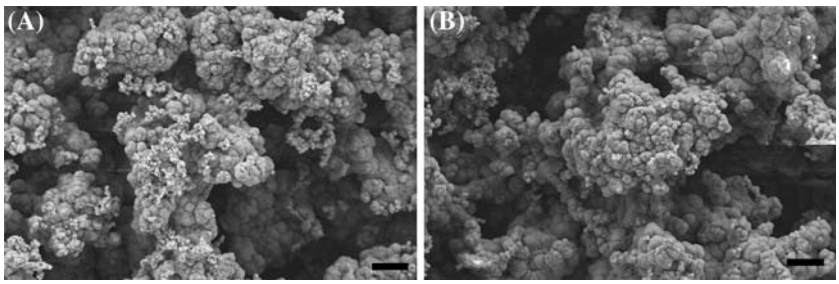

Fig. 7 SEM images of specimens after 6 weeks SBF immersion. A) anodically oxidised (bar = 10 μm), B) HA coated (bar = 10 μm)

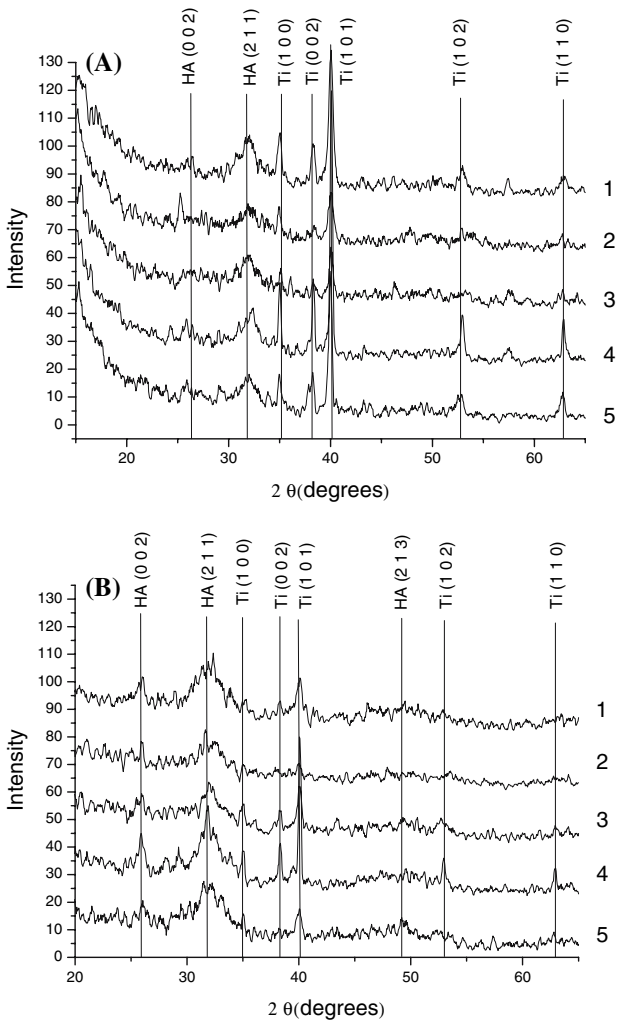

Fig. 8 XRD results of diffractograms of specimens immersed in SBF for (**A**) 4 weeks and (**B**) 6 weeks. 1: blasted titanium, 2: anodically oxidised, 3: fluoridated, 4: HA coated, and 5: alkali and heat treated. The Bragg reflections for titanium and HA are indicated

is possible to gain more knowledge of the separate processes. The qualitative and quantitative correlation of apatite formation in SBF with in vivo bone bioactivity has recently been discussed by Kokubo and Takadama [56]. After reviewing different studies on glasses, glass-ceramics, sintered hydroxyapatite and composites they concluded that there is a correlation: a material that apatite is formed on in SBF can bond to living bone through the apatite layer formed on its surface in the living body, as long as the material does not contain any substance that induces toxic or antibody reactions [56]. However, there are fewer corresponding publications for titanium.

Furthermore, during bone formation in vivo there is a circulation of blood. Studies have been performed comparing results from dynamic and static SBF models, and it was found that less calcium phosphate material was formed with the dynamic model than the static model [57]. Lu et al. [57] also found that the surface topography influence was larger in the dynamic model than in the static model. In the present study a static SBF model was used. However, the buffer was changed every week to avoid ion depletion and all specimens were treated in the same manner.

The incubation times used in this study were selected to cover the initial phase in wound healing around the implant and additionally to follow the precipitation events. This was to establish whether the crystal growth reaches a limit within the model, and also to follow and evaluate the Ca/P formation until a time point where it has been described in the literature that bone is formed. Wound healing around titanium implants is initiated by bleeding from the wound. As blood comes in contact with an implant surface it absorbs ions and proteins [58]. After a few days a fluid phase is built up around the implant, as shown by in vivo bone remodelling studies. It has been reported that the initial fluid phase decreases with time and is replaced by tissue [59–61]. An in vivo model in rabbit bone [4, 17] demonstrated that after 4–6 weeks bone growth occurs along the upper and lower parts of the implant surface.

As a control surface, a blasted titanium surface proven to have optimal surface roughness for bone response in in vivo studies [33] was selected. Contact stylus profilometry demonstrated that all the surface preparations produced similar S_a, S_{ds}, and S_{dr} mean values. This is important when comparing different surface preparations, since a difference in bone response may be related to surface roughness. A study by Barrere et al. [29] indicated that surface roughness does not influence the immediate nucleation of calcium phosphate deposits onto Ti6Al4V surfaces. However, the further growth and mechanical

attachment of the final Ca–P deposit was favoured by a rougher topography ($R_{max} > 0.25$ μm) rather than a smoother topography ($R_{max} < 0.10$ μm). Here, the roughness of the various surfaces initially decreased after the SBF immersion; probably because the precipitate reduces the roughness of the surface. After 6 weeks of SBF immersion the roughness parameters increased due to further precipitation.

In this study, all specimens were weighed before and after SBF immersion, since it was assumed that calcium phosphate formation would increase the weight of the specimens. This would be an assessment of the amount of precipitate. In general, the weight increased with increasing immersion time, although blasted and anodically oxidised specimens seemed to lose weight due to the SBF immersion. Weight changes of alkali treated titanium immersed in SBF have been previously reported [62], and it was found that the weight increased the first 2 weeks, but was lower after 20 days immersion than after 14 days. However, in the present study a variation was found between different specimens of the same type and immersion time, which emphasises the importance of working with parallel specimens in this kind of study.

SEM showed that all surfaces were completely covered by calcium phosphates after immersion for 4 weeks. This agrees with earlier SBF studies on commercially pure titanium [63] and micro-arc oxidised titanium [28]. Furthermore, the globular structures on a compact layer with cracks reported for alkali and heat treated titanium after one month SBF immersion [27], were also seen in the present study.

The amount of titanium accessible for EDX analysis, at 7 kV accelerating voltage was monitored. After 1 and 2 weeks of SBF immersion more titanium was accessible on the blasted surfaces than the four bioactive surface types. This may indicate that the different surface preparations have different ability to initiate crystal growth. After 4 and 6 weeks of immersion, the titanium signals had almost disappeared, which reflects almost complete calcium phosphate coverage. Previously, EDX has also been used for calculation of the Ca/P ratio in order to estimate the relative prevalence of amorphous and crystalline calcium phosphates [25, 26]. The stoichiometric Ca/P atomic ratios of octacalcium phosphate ($Ca_8H_2(PO_4)_6 \times 5H_2O$), tricalcium phosphate ($Ca_3(PO_4)_2$), and hydroxyapatite ($Ca_5(PO_4)_3OH$) are 1.33, 1.5, and 1.67, respectively. Takadama et al. [25] used transmission electron microscopy with energy dispersive X-ray spectroscopy (TEM/EDX) and found a Ca/P ratio of 1.40 for alkali and heat treated titanium immersed in SBF for 36 h, and an increase of the Ca/P ratio to 1.65 after 72 h of immersion. Kim et al. [26] reported similar results. In the present study the Ca/P mean ratio of alkali and heat treated specimens immersed in SBF for 1 week was 1.8. However, the Ca/P ratio varied between different areas within the same specimens.

XRD has earlier been used to study the crystallinity of calcium phosphates formed on titanium specimens after SBF immersion. Song and co-workers identified distinct apatite peaks at micro-arc oxidised titania after 28 days of SBF immersion [28]. Apatite peaks have been detected on alkali and heat treated titanium after 1 week of SBF immersion [34]. However, Lu and Leng [27] also investigated the formation of calcium phosphates in SBF on alkali and heat treated titanium. They interpreted their result as if octacalcium phosphate and not hydroxyapatite directly nucleates from amorphous calcium phosphate. They also pointed out that the P-XRD patterns of hydroxyapatite and octacalcium phosphate are alike in the 2θ range of 20–40°.

Our XRD analyses indicated the presence of hydroxyapatite crystals after both 4 and 6 weeks SBF immersion. However, after 4 weeks there was also amorphous material present, as indicated by the slope at low degrees. Furthermore, after 6 weeks the peaks were narrower due to growth of the hydroxyapatite crystals. No larger differences could be detected with P-XRD between the different surface types after 4 and 6 weeks SBF immersion.

In conclusion, differences appeared at the early SBF immersion times of 1 and 2 weeks between controls and bioactive surface types, as well as between different bioactive surface types. However, the impact on bone binding mechanisms is unclear until more studies demonstrate the correlation between in vitro and in vivo results.

Acknowledgements The authors thank Christian Erneklint at the Dept of Prosthetic Dentistry/Dental Technology, Göteborg University for kindly heat treating the alkali specimens. The authors also thank the Swedish Medical Research Council, Hjalmar Svensson Research Foundation, Knut and Alice Wallenberg Foundation, the Wilhelm and Martina Lundgren Science Foundation, the Royal Society of Arts and Sciences in Göteborg, and the Biochallenge Project from the Ministry of Science and Technology of Korea and MediSci Tec Inc (Korea) for financial support.

References

1. T. ALBREKTSSON and A. WENNERBERG, *Int. J. Prosthodont.* **17** (2004) 536
2. L. L. HENCH, *Handbook of Bioactive Ceramics*, CRC press, Boca Raton, 1990, p. 7
3. J. F. OSBORN and H. NEWESLY, *Dental Implants, Materials and Systems,* Hanser verlag, Wien, 1980, p. 111
4. L. SENNERBY, P. THOMSEN and L. E. ERICSON, *J. Mater. Sci.: Mater. Med.* **4** (1993) 240
5. C. CLOKIE and H. WARSHAWSKY, *Int. J. Oral Maxillofac.* **10** (1995) 155
6. J. E. DAVIES, B. LOWENBERG and A. SHIGA, *J. Biomed. Mater. Res.* **24** (1990) 1289
7. A. PIATTELLI, A. SCARANO and M. PIATTELLI, *Biomaterials* **16** (1995) 1333

8. A. NANCI, G. F. MCCARTHY, S. ZALZAL, C. M. L. CLOKIE, H. WARSHAWSKY and M. D. MCKNEE, *Cells Mater.* **4** (1994) 1
9. D. A. PULEO and A. NANCI, *Biomaterials* **20** (1999) 2311
10. B. D. BOYAN, *Titanium in Medicine,* Springer-Verlag, Berlin Heidelberg, Berlin, 2001, p. 561
11. T. ALBREKTSSON, P. I. BRÅNEMARK, H. HANSSON, B. IVARSSON and U. JÖNSSON, *Adv. Biomater.* **5** (1982) 167
12. L. LINDER, T. ALBREKTSSON, P. I. BRÅNEMARK, H. A. HANSSON, B. IVARSSON, U. JÖNSSON and I. LUNDSTRÖM, *Acta Orthop. Scand.* **54** (1983) 45
13. C. LARSSON, M. ESPOSITO, H. LIAO and P. THOMSEN, *Titanium in Medicine*, Springer-Verlag, Berlin Heidelberg, Berlin, 2001, p. 587
14. L. SENNERBY, P. THOMSEN and L. E. ERICSON, *J. Mater. Sci.: Mater. Med.* **3** (1992) 262
15. L. LINDER, *Acta Orthop. Scand.* **56** (1985) 269
16. P. THOMSEN and L. ERICSON, *Biomaterials* **6** (1985) 421
17. L. SENNERBY, P. THOMSEN and L. E. ERICSON, *J. Mater. Sci. Mater. Med.* **4** (1993) 494
18. T. ALBREKTSSON and H. A. HANSSON, *Biomaterials* **7** (1986) 201
19. C. JOHANSSON, J. LAUSMAA, M. ASK, H. A. HANSSON and T. ALBREKTSSON, *J. Biomed. Eng.* **11** (1989) 3
20. Y. AYUKAWA, F. TAKESHITA, T. INOUE, M. YOSHINARI, M. SHIMONO, T. SUETSUGU and T. TANAKA, *J. Biomed. Mater. Res.* **41** (1998) 111
21. P. THOMSEN, C. LARSSON, L. E. ERICSON, L. SENNERBY, J. LAUSMAA and B. KASEMO, *J. Mater. Sci.: Mater. Med.* **8** (1997) 653
22. J. D. DE BRUIJN, C. P. A. T. KLEIN, K. DE GROOT and C. A. VAN BLITTERSWIJK, *J. Biomed. Mater. Res.* **26** (1992) 1365
23. T. KOKUBO, H. KUSHITANI, S. SAKKA, T. KITSUGI and T. YAMAMURO, *J. Biomed. Mater. Res.* **24** (1990) 721
24. T. PELTOLA, M. PATSI, H. RAHIALA, I. KANGASNIEMI and A. YLI-URPO, *J. Biomed. Mater. Res.* **41** (1998) 504
25. H. TAKADAMA, H. M. KIM, T. KOKUBO and T. NAKAMURA, *J. Biomed. Mater. Res.* **57** (2001) 441
26. H. M. KIM, T. HIMENO, M. KAWASHITA, J. H. LE and T. KOKUBO, *J. Biomed. Mater. Res.* **67A** (2003) 1305
27. X. LU and Y. LENG, *Biomaterials* **25** (2004) 1779
28. W. H. SONG, Y. K. JUN, Y. HAN and S. H. HONG, *Biomaterials* **25** (2004) 3341
29. F. BARRERE, M. M. E. SNEL, C. A. VAN BLITTERSWIJK, K. DE GROOT and P. LAYROLLE, *Biomaterials* **25** (2004) 2901
30. P. PREDECKI, B. A. AUSLENDER, J. E. STEPHAN, V. L. MOONEY and C. STANITSKI, *J. Biomed. Mater. Res.* **6** (1972) 401
31. K. GOTFREDSEN, A. WENNERBERG, C. JOHANSSON, L. TEIL SKOVGAARD and E. HJORTING-HANSEN, *J. Biomed. Mater. Res.* **29** (1995) 1223
32. J. E. FEIGHAN, V. M. GOLDBERG, D. DAVY, J. A. PARR, and S. STEVENSON, *J. Bone Joint Surgery* **77** (1995) 1380
33. A. WENNERBERG, T. ALBREKTSSON, B. ANDERSSON, and J. J. KROL, *Clin. Oral Impl. Res.* **6** (1995) 24
34. L. F. COOPER, *J. Prosthet. Dent.* 84 (2000) 522
35. A. WENNERBERG, T. ALBREKTSSON and B. ANDERSSON, *J. Mater. Sci.: Mater. in Med.* **6** (1995) 302
36. A. WENNERBERG, T. ALBREKTSSON and J. LAUSMAA, *J. Biomed. Mater. Res.* **30** (1996) 251
37. A. WENNERBERG, T. ALBREKTSSON, C. JOHANSSON and B. ANDERSSON, *Biomaterials* **17** (1996) 15
38. W.Q. YAN and J. E. DAVIES, *Bioceramics* 11, World Scientific Publishing Co., New York, 1998, p. 659
39. H. B. WEN, Q. LIU, J. R. DE WIJN, K. DEGROOT and F. Z. CUI, *J. Mater. Sci.: Mater. Med.* **9** (1998) 121
40. H. M. KIM, T. KOKUBO, S. FUJIBAYASHI, S. NISHIGUSHI and T. NAKAMURA, *J. Biomed. Mater. Res.* **52** (2000) 553
41. C. APARICIO, F. J. GIL, J. A. PLANELL and E. ENGEL, *J. Mater. Sci.: Mater. Med.* **13** (2002) 1105
42. H. M. KIM, F. MIYAJI, T. KOKUBO and T. NAKAMURA, *J. Mater. Sci.: Mater. Med.* **8** (1997) 341
43. Y. T. SUL, C. JOHANSSON, E. BYON and T. ALBREKTSSON, *Biomaterials* **26** (2005) 6720
44. J. E. ELLINGSEN, *J. Mater. Sci. Mater. Med.* **6** (1995) 749
45. M. GOTTLANDER, T. ALBREKTSSON and L. V. CARLSSON, *Int. J. Oral Maxillofac. Implants* **7** (1992) 485
46. H. M. KIM, F. MIYAJI, T. KOKUBO and T. NAKAMURA, *J. Biomed. Mater. Res.* **32** (1996) 409
47. R. Z. LEGEROS, *Clin. Orthop. Relat. Res.* **395** (2002) 81
48. Y. T. SUL, C. B. JOHANSSON, S. PETRONIS, A. KROZER, Y. JEONG, A. WENNERBERG and T. ALBREKTSSON, *Biomaterials* **23** (2002) 491
49. J. E. ELLINGSEN, C. B. JOHANSSON, A. WENNERBERG and A. HOLMÉN, *Int. J. Oral Maxillofac. Implants* **19** (2004) 659
50. H. M. KIM, F. MIYAJI, T. KOKUBO, S. NISHIGUCHI and T. NAKAMURA, *J. Biomed. Mater. Res.* **45** (1999) 100
51. Y. T. SUL, C. B. JOHANSSON, Y. JEONG and T. ALBREKTSSON, *Med. Eng. Phys.* **23** (2001) 329
52. Y. T. SUL, C. JOHANSSON, A. WENNERBERG, L. R. CHO, B. S. CHANG and T. ALBREKTSSON, *Int. J. Oral Maxillofac. Implants* **20** (2005) 349
53. A. OYANE, H. M. KIM, T. FURUYA, T. KOKUBO, T. MIYAZAKI and T. NAKAMURA, *J. Biomed. Mater. Res.* **65A** (2003) 188
54. K. J. STOUT, P. J. SULLIVAN, W. P. DONG, E. MAINSAH, N. LUO, T. MATHIA and H. ZAHOUANI, *The Development of Methods for Characterisation of Roughness in Three Dimensions. EUR 15178 EN of commission of the European Communities*, University of Birmingham, Birmingham, 1993
55. A. J. VANDER, J. H. SHERMAN and D. S. LUCIANO, *Human Physiology The Mechanisms of Body Function*, 5th ed., McGraw-Hill Publishing Company, New York, 1990, p. 349
56. T. KOKUBO and H. TAKADAMA, *Biomaterials* **27** (2006) 2907
57. X. LU, Y. LENG, X. ZHANG, J. XU, L. QIN and C. CHAN, *Biomaterials* **26** (2005) 1793
58. J. M. COURTENY, N. LAMBA, S. SUDURAM and C. FORBES, *Biomaterials* **15** (1994) 737
59. A. ERIKSSON, L. L. ERICSSON, P. THOMSEN and R. LINDBLAD, *J. Mater. Sci. Mater. Med.* **5** (1994) 269
60. A. ROSEZGREN, B. JOHANSSON, N. DANIELSEN, P. THOMSEN and L. ERICSON, *Biomaterials* **17** (1996) 1779
61. T. MASUDA, G. SALVI, S. OFFENBACHER, D. FELTON and L. COOPER, *Int. J. Oral Maxillofac. Impl.* **12** (1997) 472
62. L. JONASOVA, F. A. MULLER, A. HELEBRANT, J. STRNAD and P. GREIL, *Biomaterials* **25** (2004) 1187
63. P. LI and P. DUCHEYNE, *J. Biomed. Mater. Res.* **41** (1998) 341